ELSEVIER

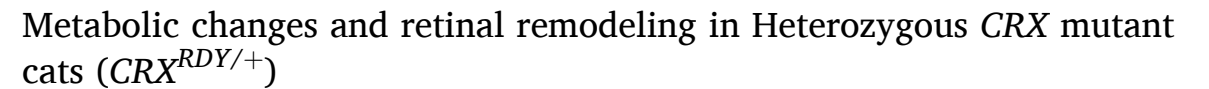
Contents lists available at ScienceDirect

Experimental Eye Research

journal homepage: www.elsevier.com/locate/yexer



Research article





- a Small Animal Clinical Sciences, Michigan State University, 736 Wilson Road, East Lansing, MI, USA
- ^b Ophthalmology, Moran Eye Center, University of Utah, Salt Lake City, UT, USA

ARTICLE INFO

Keywords:
CRX
Leber congenital amaurosis
Large-animal model
Cat
Retinal degeneration
SD-OCT
Immunohistochemistry
Computation molecular phenotyping

ABSTRACT

CRX is a transcription factor essential for normal photoreceptor development and survival. The CRX^{Rdy} cat has a naturally occurring truncating mutation in CRX and is a large animal model for dominant Leber congenital amaurosis. This study investigated retinal remodeling that occurs as photoreceptors degenerate. $CRX^{Rdy/+}$ cats from 6 weeks to 10 years of age were investigated. In vivo structural changes of retinas were analyzed by fundus examination, confocal scanning laser ophthalmoscopy and spectral domain optical coherence tomography. Histologic analyses included immunohistochemistry for computational molecular phenotyping with macromolecules and small molecules. Affected cats had a cone-led photoreceptor degeneration starting in the area centralis. Initially there was preservation of inner retinal cells such as bipolar, amacrine and horizontal cells but with time migration of the deafferented neurons occurred. Early in the process of degeneration glial activation occurs ultimately resulting in formation of a glial seal. With progression the macula-equivalent area centralis developed severe atrophy including loss of retinal pigmentary epithelium. Microneuroma formation occurred in advanced stages as more marked retinal remodeling occurred. This study indicates that retinal degeneration in the $Crx^{Rdy/+}$ cat retina follows the progressive, phased revision of retina that have been previously described for retinal remodeling. These findings suggest that therapy dependent on targeting inner retinal cells may be useful in young adults with preserved inner retinas prior to advanced stages of retinal remodeling and neuronal cell loss.

1. Introduction

Cone-rod homeobox (*CRX*) is an *OTX*-like homeobox gene encoding a transcription factor essential for normal photoreceptor development, function and homeostasis (Furukawa et al., 1999; Hennig et al., 2008). *CRX* mutations result in a spectrum of dominant retinopathies ranging from Leber congenital amaurosis (LCA) to cone–rod dystrophy (CoRD), retinitis pigmentosa (RP) and macular degeneration (MD). The *CRX*^{Rdy} cat has a spontaneous frameshift mutation in *CRX* (c.546del, p. Ala185leuTer2) and is a model for severe dominant Leber congenital amaurosis (Curtis et al., 1987; Leon and Curtis, 1990; Leon et al., 1991; Menotti-Raymond et al., 2010; Occelli et al., 2016). The *Rdy* (rod-cone dysplasia – which is actually a misnomer) mutation is classified as a Class III *CRX* mutation which are those which have antimorphic frameshift/nonsense mutations with intact DNA binding (Tran and Chen, 2014). The mutant *Rdy* protein is expressed and has a functional DNA binding domain but disrupted transactivation site. It accumulates to

abnormal levels disrupting normal expression of target photoreceptor genes. Affected animals have a halted development of photoreceptors followed by a progressive retinal degeneration starting in the macula-equivalent retinal region, the area centralis (Occelli et al., 2016).

Retinal remodeling occurs as photoreceptors begin to exhibit stress and subsequent cell death, and has been described in rodent models and human subjects (Jones et al., 2003). During and following photoreceptor loss deafferented inner retinal neurons can undergo cell death or neuronal sprouting and rewiring. Glial activation occurs early in the course of retinal degeneration with Müller glia being some of the first cells that respond to cell stress (Pfeiffer et al., 2016, 2019, 2020). Ultimately, Müller glia are involved in a glial scar sealing the remaining neurons. The major changes to inner retinal circuitry and glia with a variety of retinal dystrophies have been described in detail (Jones et al., 2012, 2016a, 2016b; Jones and Marc, 2005; Marc and Jones, 2003; Marc et al., 2003). These major neuronal changes have implications for

^{*} Corresponding author. Small Animal Clinical Sciences, Michigan State University, East Lansing, MI, 48824, USA.

E-mail addresses: l_occelli@yahoo.fr (L.M. Occelli), bryan.jones@m.cc.utah.edu (B.W. Jones), taylorj.cervantes@gmail.com (T.J. Cervantes), peter315@msu.edu (S.M. Petersen-Jones).

therapies such as transplantation, and prostheses aiming to restore vision after photoreceptor loss.

Over the last 20 years, the use of amino acid retinal signatures has been developed and used to investigate retinal remodeling resulting from inherited and acquired retinal diseases (Jones and Marc, 2005; Jones et al., 2003; Marc and Jones, 2003; Marc et al., 2003). Fourteen separable biochemical theme classes have been identified: photoreceptor, bipolar and ganglion cells characterized by specific glutamate signature, amacrine cells by glycine and gamma-aminobutyric acid (GABA) signature, horizontal cells by GABA signature, Müller cells by taurine-glutamine signature and retinal pigmentary epithelium (RPE) cells by an aspartate-glutamate-taurine-glutamine signature. The rest of the cells which fill the neuronal space, present with glutamate, GABA, or glycine signatures. While amino acid retinal signatures have been described in normal and detached cat retinas, they have not been described in large animal models of retinal dystrophies (Marc et al., 1998a, 1998b).

The purpose of this study was to investigate the timing and extent of retinal remodeling during retinal degeneration in the $CRX^{Rdy/+}$ cat. This information will be important for assessing the stages of the disease process that may be amenable to different translational therapies such as retinal transplantations, retinal prosthesis or optogenetics.

2. Materials and methods

2.1. Ethics statement

All procedures were performed in accordance with the ARVO statement for the Use of Animals in Ophthalmic and Vision Research and approved by the Michigan State University Institutional Animal Care and Use Committee.

2.2. Animals

Heterozygous mutant $CRX^{Rdy/+}$ cats and wild-type (WT) control cats maintained within a colony at Michigan State University housed under a 12L:12D cycles (facility light level $\sim 8 \times 10^3$ lux), were studied. They received commercial feline dry diet (Purina One Smartblend and Purina Kitten Chow, Nestlé Purina, St Louis, MO. USA). Cats were studied during retinal maturation and adulthood from 4 weeks to 10 years of age. Supplementary Table S1 shows the numbers of animals used.

2.3. In vivo ophthalmic examination and fundus imaging

In vivo ophthalmic fundus and retinal changes were investigated by ophthalmic examination, fundus photography (Ret-Cam II, Clarity Medical Systems, Inc., Pleasanton, CA, USA), confocal scanning laser ophthalmoscopy (cSLO) including autofluorescence imaging (AF) and spectral domain – optical coherence tomography (SD-OCT) (Spectralis OCT + HRA, Heidelberg Engineering Inc., Heidelberg, Germany) as previously described (Occelli et al., 2016). Fluorescein angiography was performed as previously described (Occelli et al., 2022).

SD-OCT single scan line and volume scan images were recorded from the center of the *area centralis* and from the four retinal quadrants (at 4 optic nerve head distances from the edge of the optic nerve head superiorly, inferiorly, nasally and temporally (Fig. S1). Total retinal thickness, Receptor+ (REC+; representing the length of the photoreceptor from outer plexiform layer to retinal pigment epithelium) (Hood et al., 2009), inner nuclear layer (INL), ganglion cell complex (GCC; including the inner plexiform layer (IPL) and the ganglion cell layer (GCL)) and inner retina (IR; layers from internal limiting membrane to inner nuclear

layer) thickness were measured (Fig. S1) using the Heidelberg Eye Explorer (HEYEX) software.

2.4. Retinal histology

Retinal changes were investigated using immunohistochemistry (IHC), plastic embedded thin sections and computational molecular phenotyping (CMP).

2.4.1. Frozen section immunohistochemistry (IHC)

After euthanasia, eyes were processed for cryosectioning for IHC as previously described (Mowat et al., 2014; Occelli et al., 2016). The antibodies used are listed in Supplementary Table S2.

2.4.2. Plastic embedded sections

Eyes were glutaraldehyde fixed as previously described (Occelli et al., 2016). Retinal samples were collected from 5 different regions (Supplementary Fig. S2.) and epoxy-embedded: area centralis (AC), superior mid- and far-periphery (SupMP, SupFP), and inferior mid- and far- periphery (InfMP, InfFP) to investigate regional differences. ONL, INL and GCC cells were counted on 3 different 1 μm sections for each time point (same area/same animal) and on a 100 μm width for each area.

2.4.3. CMP for macromolecules and small molecules (CMP)

Eyes as previously fixed in mixed aldehyde buffers for regular histologic sections were used for CMP analysis. Retinas were collected from 5 different areas of the fundus (Supplementary Fig. S1) and epoxyembedded: *area centralis* (AC), superior mid- and far-periphery (SupMP, SupFP) and inferior mid- and far- periphery (InfMP, InfFP) to investigate regional differences. 200 nm serial retinal sections were assessed.

CMP was performed as previously described (Marc et al., 1995). With samples being processed for macromolecules and small molecules (CMP) including GABA (yy), glycine (G), L-glutamate (E), taurine (TT), L-glutamine (Q), glutathione red ox (J), L-aspartate (D), L-arginine (R), red-green opsin (RGO), rhodopsin (1D4), cellular retinaldehyde binding protein (CRALBP), and glutamine synthetase (GS) (for the antibodies list and dilution refer to (Jones et al., 2016b)). CMP data were visualized with secondary antibodies conjugated to 1.4 nm gold, followed by silver intensification and image capture and processing as previously described (Marc and Jones, 2002; Marc et al., 1995). Molecular signals were visualized as RGB maps using red, green, and blue for example respectively TQE: Taurine red, L-Glutamine green, L-Glutamate E blue, YGE: GABA γ red, glycine G green, glutamate E blue.

2.5. Statistical analysis

A mixed effect model using R studio was used to analyze the data for SD-OCT and measurements as data was evaluated over time. The equation below was used (RStudio Team (2015). RStudio: Integrated Development for R. RStudio).

$$Y_i = \sum_{i=0}^n \beta X + \alpha_i + \varepsilon_i$$

where β is the parameter vector. X is the independent variable matrix, α_i is the cat level residual, and the \mathcal{E}_i is the individual observation level residual.

No statistical analysis was performed for the cell nuclei counting as only a n of 1 was available for most of the ages and there was a lack of

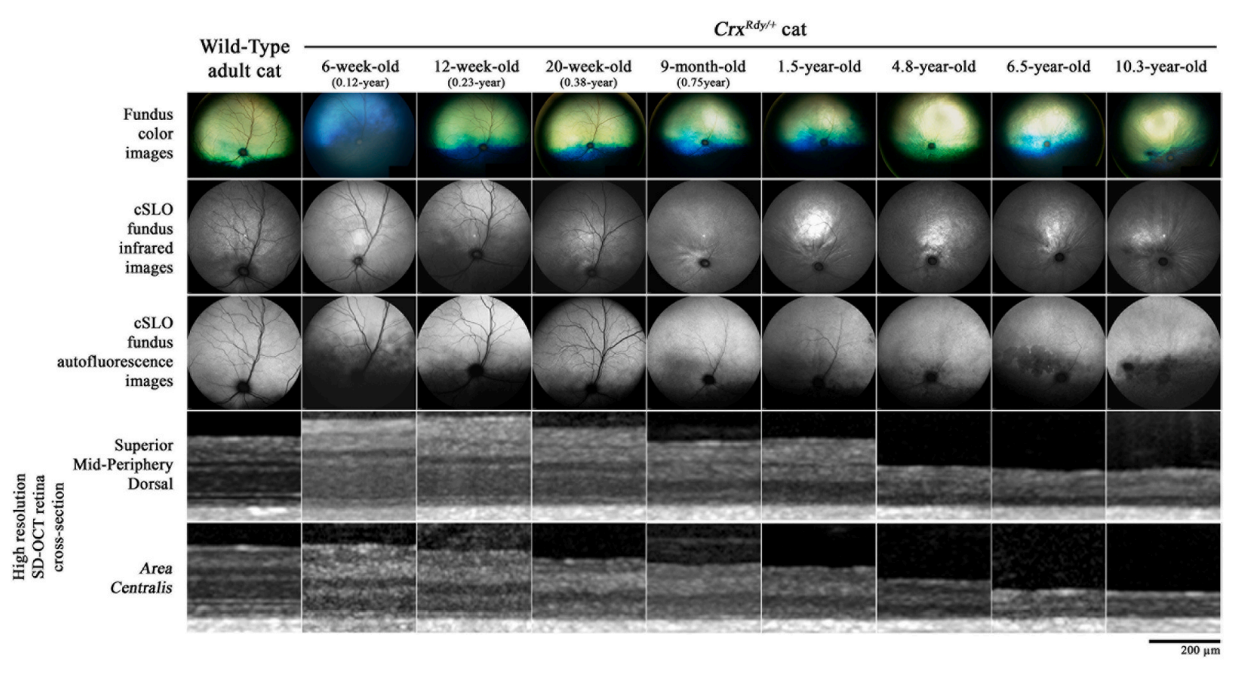


Fig. 1. Fundus and morphological changes in the *CRX*^{Rdy/+} cat with age. **Color fundus images**. Superficial retinal vascular attenuation was noticeable as early as 20-weeks of age and obvious by 9-months of age. Tapetal fundus hyperreflectivity was noticeable in the region of the *area centralis* at 12-weeks of age (in this panel) then became more generalized by 20-weeks of age. Color fundus images also showed that by 6.5- and 10.3-years of age a lesion in the region of the *area centralis* had developed. **Infrared cSLO fundus images**. Those images demonstrate the vascular attenuation that occurred with disease progression and was very marked after 20-weeks of age. **Autofluorescence cSLO fundus images**. Similarly to the color and infrared cSLO images, images illustrate the vascular attenuation that develops. They also show the development of a lesion seen as a decrease in fundus autofluorescence in the region of the *area centralis* and extending along the visual streak in the 6.5- and 10.3-year-old affected cats. The lesion was most severe in the10.3-year-old affected cat where there was a complete lack of fundus autofluorescence in the *area centralis*. **High resolution cross-section SD-OCT images of the dorsal (Sup Mid-Periphery) and** *area centralis* **regions. The ellipsoid and interdigitation zones on SD-OCT are not detectable in the affected cats at any age examined. They initially developed a thinning of the outer retina with apparent loss of the outer nuclear layer from 9-months of age. The inner retina initially thickened then thinned in the later stages of disease. Retinal thinning was apparent initially in the** *area centralis* **(from as early as 6 weeks of age).**

age-matched WT controls.

3. Results

3.1. CRX^{Rdy/+} cats develop a severe retinal degeneration starting in the area centralis

In vivo fundus imaging (color, infrared and AF cSLO and SD-OCT) was used to investigate the natural history of retinal degeneration in the $CRX^{Rdy/+}$ cat (Fig. 1). As early as 7 weeks of age, on fundoscopy, tapetal hyperreflectivity (an indicator of retinal thinning) was present in the area centralis, and then in the rest of the fundus by 20 weeks of age. Attenuation of the superficial retinal blood vessels was noticeable as early as 20-weeks of age and worsened with disease progression. By 6.5 years of age some affected cats had developed a bluish appearing lesion in the area centralis. This progressed such that in the older cats the lesion appeared dark in color. On AF cSLO, the lesion showed a progressive decrease in autofluorescence until there was a complete lack of autofluorescence. With progression this lesion also extended along the visual streak (the lesion is considered further below Fig. 7).

Retinal cross-sectional imaging (SD-OCT) showed a lack of the reflective bands that represent the region of the inner and outer segments (ellipsoid and interdigitation zones) from the earliest age imaged (4 weeks of age). The suspected early retinal thinning in the *area centralis* was confirmed on SD-OCT (see lower two rows Fig. 1). Measurements of the retinal layers on SD-OCT images showed significant changes in thicknesses in all 5 regions of the retina examined (Fig. 2 and Supplementary Fig. S3). The changes were similar in all regions but more marked in the *area centralis*. The Receptor+ (REC+) and the outer nuclear layer (ONL) layer, which is part of the REC+, showed a

progressive thinning starting at an early age (as early as 6 weeks of age in the area centralis and 10/12 weeks of age in the other regions). By one year of age the REC + layer had thinned to $29.0\pm8.2~\mu m$ in the area centralis compared to $125.3\pm9.3~\mu m$ in WT controls. The inner retina (IR) underwent thickening from 20 to 26 weeks of age with this peaking at around 1 year of age. After 2 years of age the IR then became thinned as part of the severe generalized retinal degeneration (Fig. 2 and Supplementary Fig. S2). By 1 year of age, the IR thickness in the dorsal region of the $CRX^{Rdy/+}$ cat was $132.1\pm12.78~\mu m$ compared to $78.7\pm2.1~\mu m$ in the WT cat, having thickened from $107.8\pm7.9~\mu m$ at 10 weeks of age. The IR thickneing counteracted the outer retinal thinning meaning that the total retinal (TR) thickness tended to not decrease until later in the disease process. At 1 year of age, the TR thickness in the dorsal region of the $CRX^{Rdy/+}$ cat was $161.5\pm15.0~\mu m$ compared to $197.9\pm3.7~\mu m$ in the WT cat.

In order to further evaluate the changes in retinal cellular layers, we evaluated plastic sections from the five retinal regions (Fig. S2). Stunting of photoreceptor IS/OS were seen as early as 6 weeks of age and by 20 weeks of age only stunted IS remained. Counts of the number of cell nuclei of each layer in each retinal region (Fig. 3 and Supplementary Fig. S4) showed there was a severe loss of ONL nuclei during the first 6 months of life. The INL did not show major changes in nuclei numbers over that time period. This was not analyzed statistically due to the n number of only one individual for most of the time points assessed. In the *area centralis* there was a decrease of ONL nuclei from 129 ± 7.2 at 6 weeks of age to 44.7 ± 6.0 at 9 months of age (over a retinal length of $100~\mu m$). While it decreased from 270 ± 9.5 to 34 ± 2.6 in the dorsal Sup MP region. With disease progression disorganization of the retinal nuclear layers developed. The changes observed and layer thinning was more rapid in the *area centralis* region. Ganglion cells were well

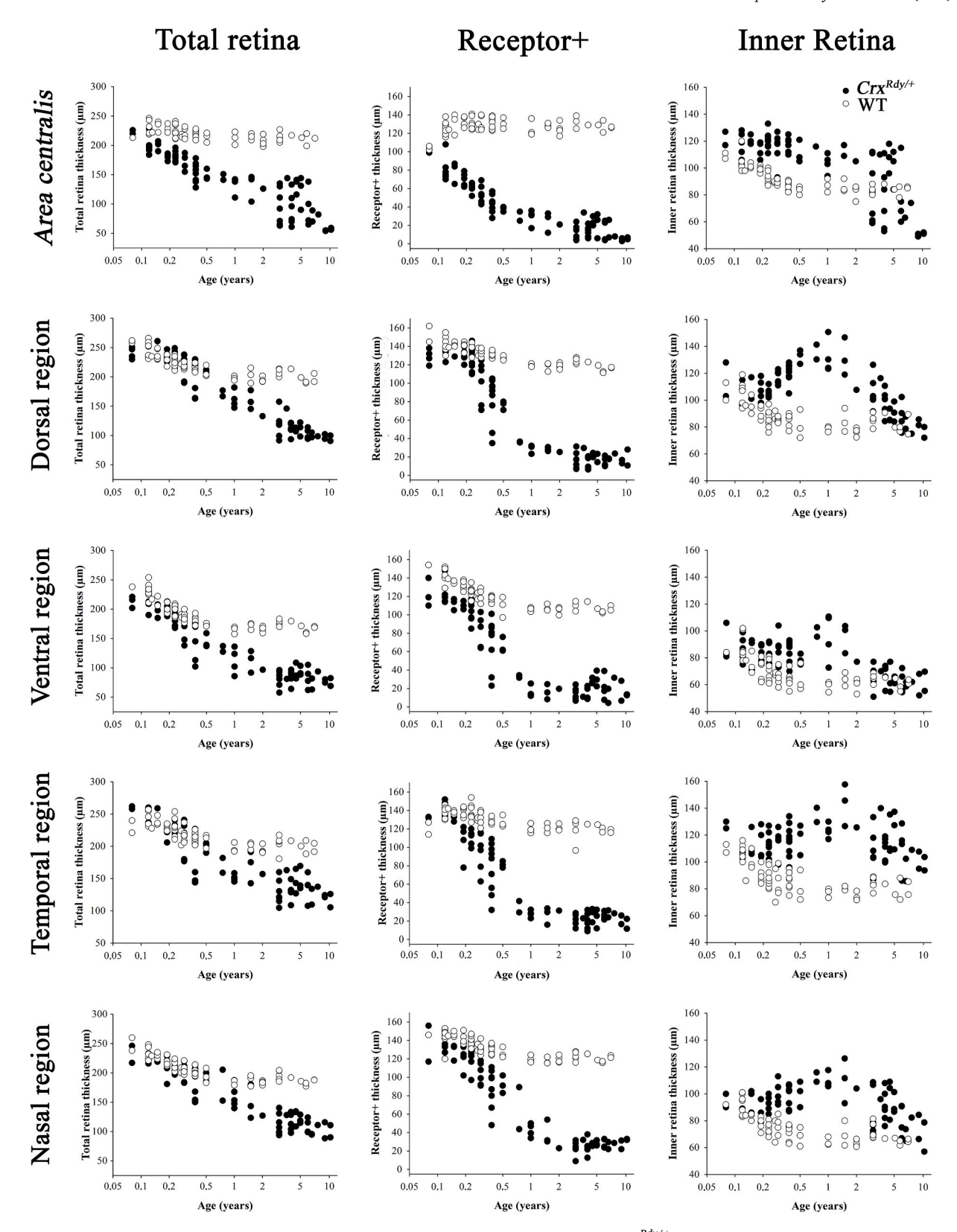
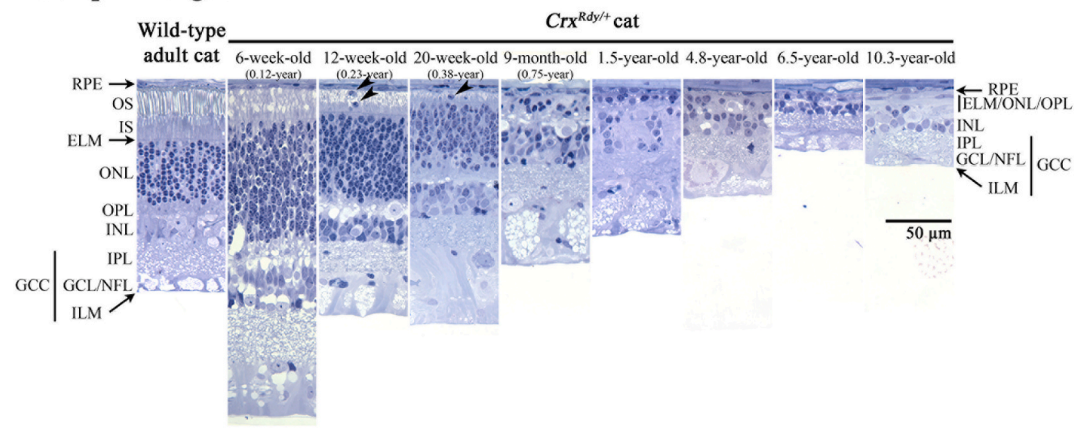


Fig. 2. Total retina (TR), Receptor+ (REC+) and Inner retina (IR) thicknesses scatter plots from $CRX^{Rdy/+}$ and WT control cats from 4 weeks to 10.25 years of age. Measures were made on SD-OCT images from the *area centralis* region and from four optic nerve head distances from the optic nerve rim itself dorsally, ventrally, temporally and nasally. The REC+, IR, and TR of WT animals thinned during the first year of age in all retinal areas except the *area centralis* where the REC + did not show thinning over the first year. After one year the layer thicknesses in WT cats remained similar for the duration of the study. In the affected animals the REC + showed early marked thinning initially starting in the *area centralis* and then involving all retinal regions. The IR initially thickneed in all regions (except for the *area centralis*) with a peak around 1–2 years of age and then thinned with the disease progression. The TR thickness decreased progressively in all retinal regions although the initial thickening in the IR tended to counteract the effect of the marked REC + thickening on TR thickness.

A. Sup MP region



B. Sup MP and AC regions: cell nuclei count - age plots

C. AC region

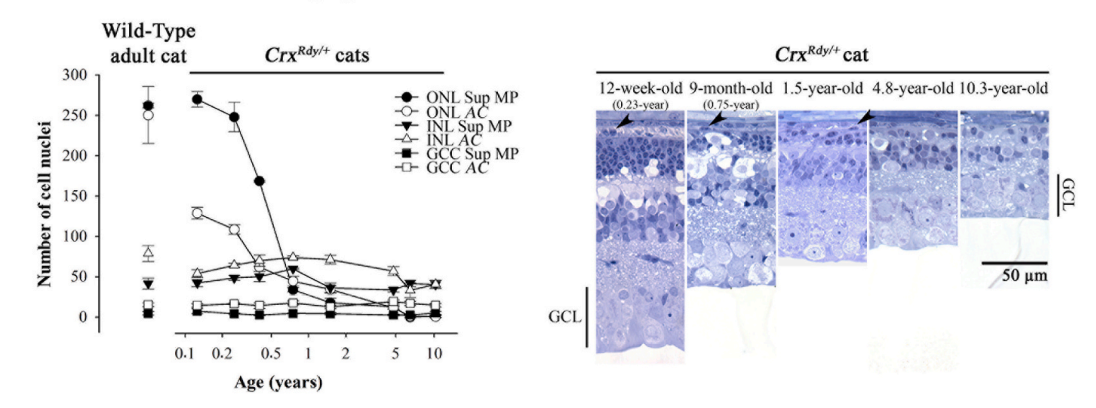


Fig. 3. Histologic images from plastic sections from (A) the Superior Mid-Periphery (Sup MP) and (C) the *area centralis* regions and (B) nuclei counts of the different retinal nuclei layers. (A) Semithin histological sections from the SupMP periphery. With age, a severe thinning of the retina could be seen in the *CRX*^{Rdy/+} cat by 20 weeks of age. Abnormal photoreceptor IS/OS were seen as early as 6 weeks of age and by 20 weeks of age only stunted IS are seen. In sections from 12 to 20 week old *CRX*^{Rdy/+} cats ectopic nuclei are seen in the subretinal space (indicated by *black arrowheads*). More extensive remodeling is seen as early as 9 months of age where disorganization of the nuclear layers becomes obvious. (B) Cell nuclei count of the ONL, INL and GCC in the Sup MP and *area centralis* regions (number of cell nuclei per 100 µm retinal section). Severe loss of ONL nuclei occurred in both regions. The *area centralis* already had reduced numbers of nuclei from the earliest age tested (6 weeks of age) compared to WT animals. Numbers of INL nuclei were well maintained initially but decreased in older animals. Ganglion cell numbers were well maintained. (C) Semithin histological sections from the *area centralis* region. Changes developed more rapidly than in the Sup MP region (A), including a more rapid layer thinning. Note that ganglion cells remain well preserved during the disease progression. Key: RPE, retinal pigment epithelium; OS, outer segments; IS, inner segments; ELM, external limiting membrane; ONL, outer nuclear layer; OPL, outer plexiform layer; INL, inner nuclear layer; IPL, inner plexiform layer; GCL, ganglion cell complex; ILM, inner limiting membrane.

preserved during the disease progression. (Fig. 3A and C).

3.2. CRX^{Rdy/+} cat retinas undergo marked retinal remodeling

To more precisely investigate the retinal changes, further histology, IHC and CMP were performed (Figs. 4-6). As detected, both on SD-OCT and plastic-embedded sections, IHC and thin sections for CMP showed that there was an early and progressive thinning of the outer retina. With inner retinal changes developing later. IHC showed that there was a rapid loss of cone immunomarkers. Labeling with human cone arrestin (hCAR, which labels all cones) was not present after 12 weeks of age (data not shown). No S-cone opsin immunoreactivity was detectable at any age. ML-cone labeling was present for longer, although it was mislocalized to the inner segments and cell bodies (Fig. 4A1), but was also progressively lost. Markers for rhodopsin on IHC (Fig. 4A2) and CMP (Fig. 5) revealed mislocalization to the inner segments (IS) and cell bodies from as early as 6 weeks of age. Rhodopsin immunolabelling decreased with age and was not detected in the older animals (Figs. 4 and 5). PKCalpha immunolabeling showed extension of rod bipolar cells into the ONL (Fig. 4B1). Müller glia activation as indicated by

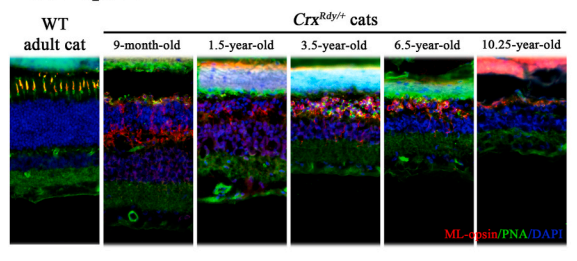
upregulation of GFAP was extensive (Fig. 4B2). Glutamate and aspartate CMP labeling was present in most cells except Müller cells which showed an increased activation with development of glial seals and columns (Fig. 5). There was migration of inner retinal cells towards both the outer retina and the ganglion cell layer as demonstrated by CMP GABA labeling of the horizontal cells, bipolar and amacrine cells and calbindin and PKC α IHC labeling. Taurine labeling showed the loss of inner-outer photoreceptor segments and indicated that most cells remaining had an inner retinal origin. CRALBP labeling was decreased from an early age. Interestingly, labeling with NeuN, a marker for neuronal cells, was increased in the $CRX^{Rdy/+}$ cat (Fig. 4B1).

TQE and YGE mapping on thin sections (Fig. 6) as well as examination of semithin histologic sections showed major remodeling with migration of inner retina cells into the outer retina through migration columns. Remodeling of inner retinal cells led to the development of microneuroma forming abnormal connection between cells. Retinal pigmentary epithelium atrophy was also noticeable on many sections (Fig. 6).

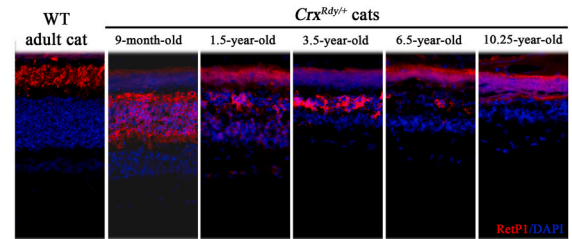
A. Photoreceptor cell markers

1. Medium-long wavelength cone marker

- ML-opsin

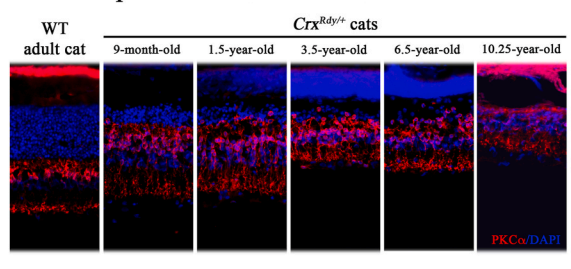


2. Rod marker - RetP1

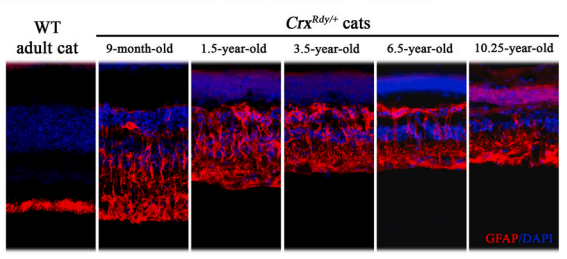


B. Inner retinal cell markers

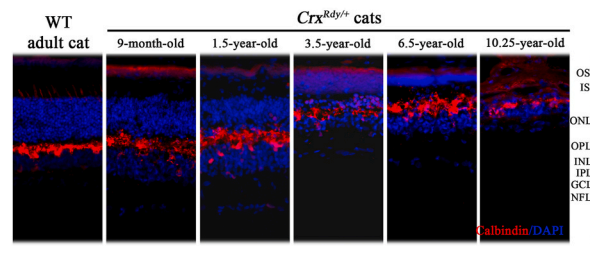
1. Rod bipolar cell marker - PKCα



2. Activated Müller cell marker - GFAP



3. Other retinal cells marler - Calbindin



4. Neuronal cell marker - NeuN

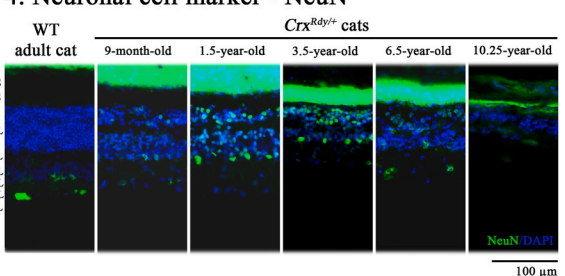


Fig. 4. Immunohistochemisty during disease progression in the $CRX^{Rdy/+}$ cat. (A) Photoreceptor cell markers. 1. ML-opsin was mislocalized to the ONL initially and then not detectable (only background is detectable). 2. Rhodopsin was similarly mislocalized to the ONL and was detectable in the ONL up to 6.5 year of age. (B) **Inner retinal cell markers. 1.** Rod bipolar cells were present in the $CRX^{Rdy/+}$ cat until later in disease progression. However, with disease progression dendrites and some of their nuclei migrated to the outer retina starting at 1.5 years of age. At older ages their dendrites became retracted and less apparent. **2.** Müller cells are highly activated and from an early age they invaded the ONL towards the subretinal space. **3.** Calbindin labeling of the inner retinal cells (horizontal cells and some cone bipolar cells) showed some moderate changes in normal staining, a sign of remodeling. Unlike in the WT control no staining of cone photoreceptor outer segments was noted. **4.** NeuN labeling showed some abnormal localization to the ONL and a more prominent labeling of the INL nuclei than in normal cat retina. Key: OS, outer segments; IS, inner segments; ONL, outer nuclear layer; OPL, outer plexiform layer; INL, inner nuclear layer; IPL, inner plexiform layer; GCL, ganglion cell layer; NFL, nerve fiber layer.

3.3. Retinal pigmentary epithelium degenerates in the area centralis of $CRX^{Rdy/+}$ cats

In addition to the generalized retinal remodeling, a focal lesion was detected on both color and autofluorescence fundus imaging in older cats (Figs. 1 and 7) as described above. This lesion was found to correspond to a loss of retinal pigmentary epithelium (RPE), detectable on both SD-OCT and IHC (Fig. 7). Some islands of remaining RPE cells could be identified with patches of RPE hypertrophy present in those areas and at the edge of the lesion. Fig. 7 shows hyperfluorescent spots on fluorescein angiography (A), thicker RPE and REC + on color thicknesses map B1 and SD-OCT (B2) and seen on histologic (B3) and IHC (B4) sections.

3.4. Other findings in individual $CRX^{Rdy/+}$ cats

Very old cats with severe degeneration developed retinal holes in their ventral retina. This could be seen either by fundus examination (fundus images) or SD-OCT retinal cross-section (Fig. 8). However, in

some areas accumulations of cells could be detected on SD-OCT and CMP histology. Small areas of retinal detachments could be seen next to the *area centralis* degeneration in SD-OCT imaging. One cat presented with retinoschisis affecting its ventral non-tapetal retinal region (Fig. 8).

4. Discussion

This study expands on previous reports showing that the *CRX*^{Rdy/+} cat has a severe, early-onset, dominantly inherited, retinal degeneration (Chong et al., 1999; Curtis et al., 1987; Leon and Curtis, 1990; Leon et al., 1991; Occelli et al., 2016). Functional evaluations were not included in this study as these have been described in detail previously. Electroretinographic studies showed an absence of cone responses with very reduced rod responses in the young animals which were lost by about 20 weeks of age (Leon et al., 1991; Occelli et al., 2016).

The *CRX*^{Rdy/+} cat had a cone-led photoreceptor degeneration. Immunostaining for S-opsin failed to detect any immunopositive photoreceptors at any age. ML cone opsin was present but mislocalized to the residual inner segment and cell body. In keeping with the previously

Amino acid signatures in the central retina of $Crx^{Rdy/+}$ cats 6-week-old 20-week-old 5-year-old 10-year-old

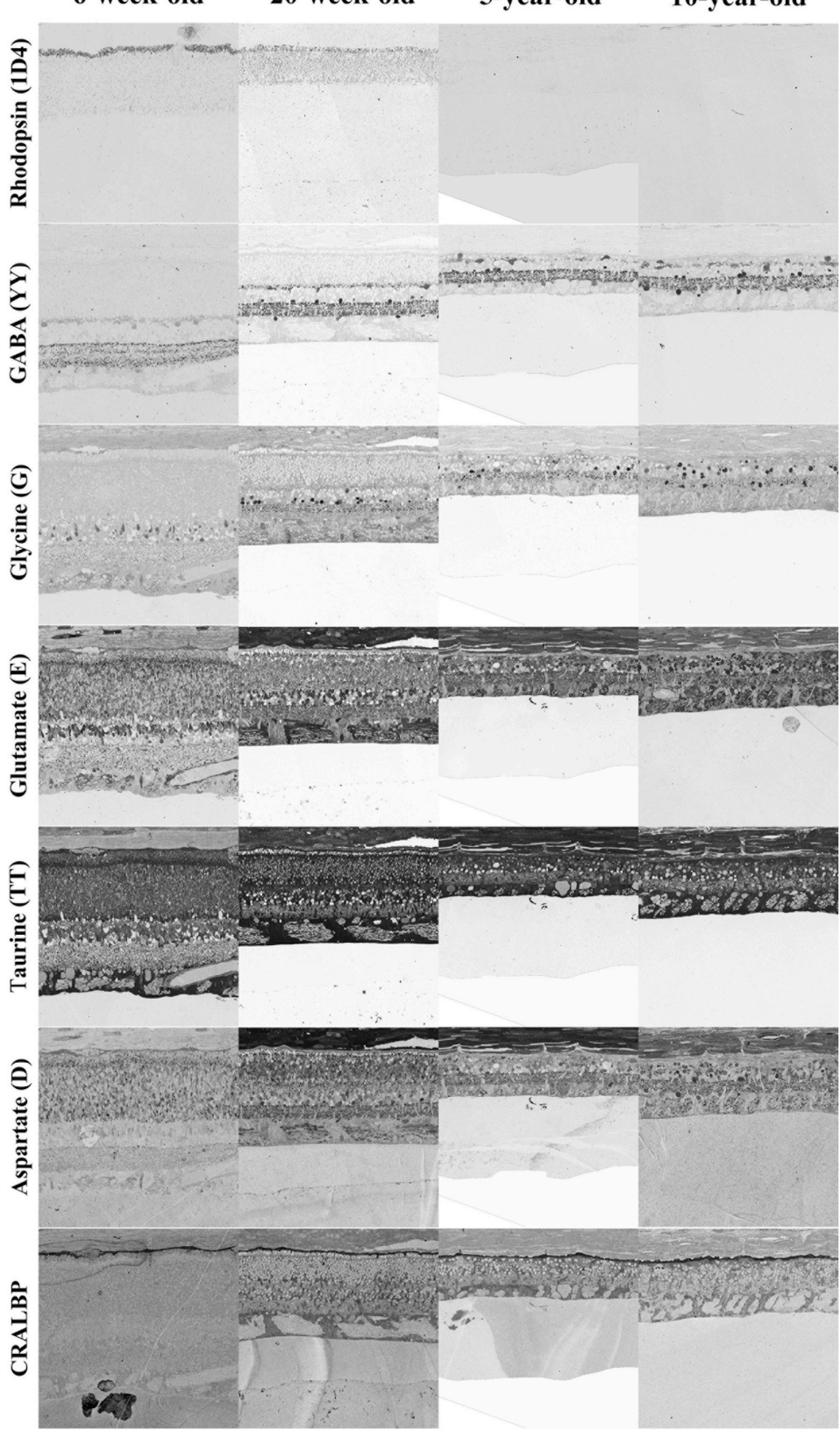


Fig. 5. Retinal amino acid signatures in 6week, 20-week, 5-year and 10-year-old CRXRdy/+ cats. Serial 200 nm sections in the superior mid-periphery (SupMP; central retina). There was significant retinal thinning over time, with some individual variation at later ages. The outer nuclear layer was the first to thin then the inner retina. Rhodopsin labeling decreased with age and became extensively mislocalized to the rod inner segments and somas, then disappeared at ~5 years of age. GABA labeled horizontal, bipolar and amacrine cells migrated both towards the outer retina and the ganglion cell layer. Glutamate and aspartate labeling was present in most cells except Müller cells which showed an increased activation with development of glial seals and columns. Taurine labeling showed the loss of inner-outer photoreceptor segments and that most cells remaining had an inner retinal origin. CRALBP labeling was decreased from an early age.

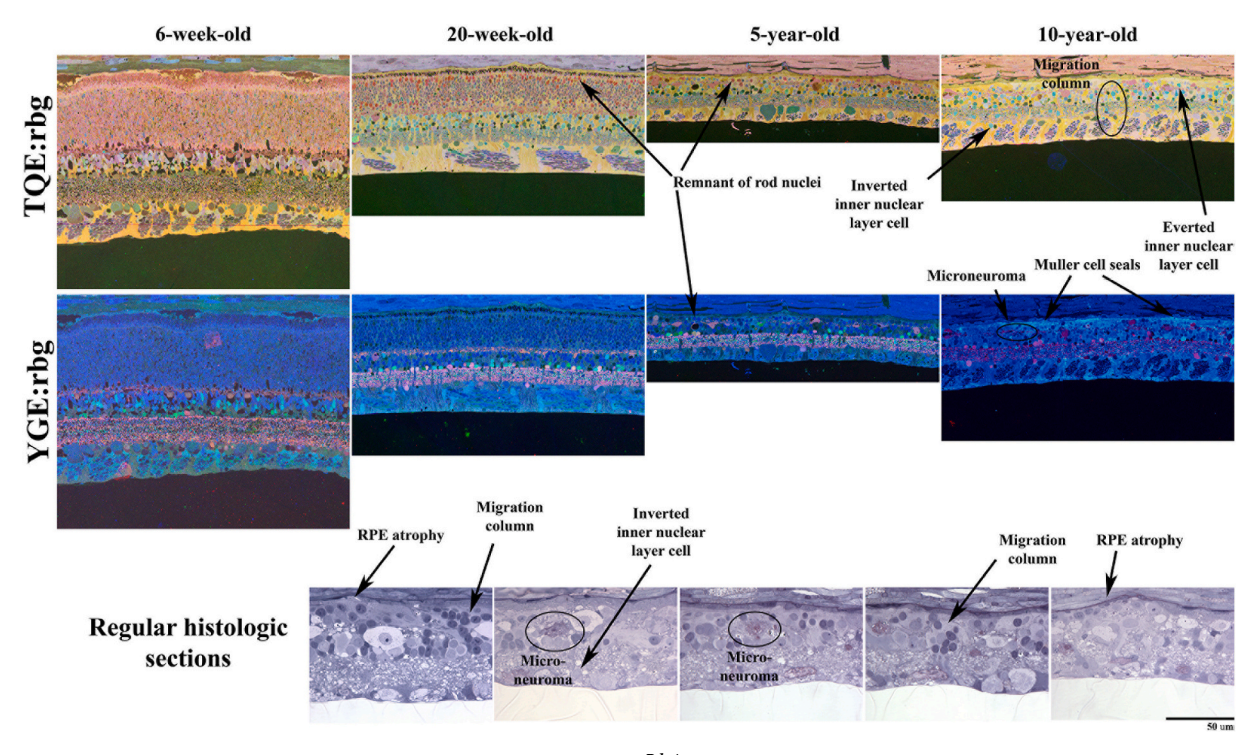


Fig. 6. TQE and YGE CMP mapping and semithin histologic sections in the $CRX^{Rdy/+}$ cat at different ages in the superior mid-periphery area (central retina) and 1 μ m epoxy-embedded semithin sections from dorso-central retinal samples (from 5- and 10-year-old animals). This figure displays the different stages of degeneration and remodeling with loss of photoreceptor outer and inner segments then death with Müller cell activation then hypertrophy. With disease progression, migration columns appeared, inverted and everted inner nuclear cells as well as microneuromas and RPE atrophy.

reported presence of some rod ERG responses, rhodopsin immunolabelling was present, but only rudimentary rod outer segments were present in young animals and these were rapidly lost. Rhodopsin mislocalization occurred as photoreceptors degenerated. The degeneration of photoreceptors resulted in early thinning of the outer retinal layers. This started in and was most severe in the area centralis which is the macula-equivalent retinal region of the cat. Eventually RPE was also lost in this region with some patches of RPE hypertrophy developing at the edge of the lesion. This recapitulates the phenotype of CRX-associated retinopathies in humans (Freund et al., 1997; Huang et al., 2012). Macular degeneration is reported in humans with some CRX mutations and further supports the fact that the cat is a valuable model for the human form of the disease (Itabashi et al., 2003, 2004; Nishiguchi et al., 2020). The presence of a macula-equivalent region and a human sized eye means that the cat model provides specific advantages over the laboratory rodent Crx-mutant models. Although degeneration started in the area centralis in the CRXRdy/+ cat, all retinal regions were also affected.

With loss of photoreceptors, the inner retina, as measured by SD-OCT, initially thickened, corresponding in timing to Müller glia activation. Despite the outer retinal thinning this meant that the total retinal thickness remained virtually unchanged until 6 months of age, after which it also decreased. With disease progression extensive retinal remodeling developed. This was similar to that previously described in inherited retinal dystrophies in other species (Jones et al., 2003, 2012, 2016a, 2016b; Jones and Marc, 2005; Marc and Jones, 2003; Marc et al., 2003). Detailed studies of retinal remodeling described 3 phases of the process (Jones et al., 2012, 2016a). During the first phase of remodeling, the photoreceptors undergo stress and in the case of the *CRX*^{Rdy/+} cat incomplete development then death corresponding with the start of the second phase of remodeling. During the second phase, Müller cells are

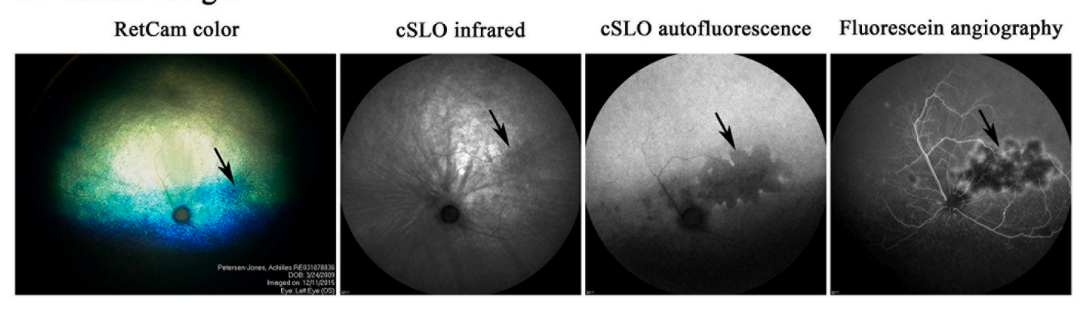
activated and eventually form glial seals encasing the residual retinal neurons. Inner retinal neurons undergo marked changes including hypertrophy and extension of horizontal cell neurites and changes to bipolar cell dendrites which initially extend into the ONL and then appear to retract with further remodeling. During the third phase of remodeling, the glial seal became fibrotic and Müller cell hypertrophic. Neuronal cells start dying and microneuromas form. In the $CRX^{Rdy/+}$ cat, the first phase of this remodeling process occurs during the first few weeks of age. The second phase is also rapid; occurring over the first months of age. By 1.5-years of age, the inner retina is severely affected and by 5-years of age severe neuronal remodeling has developed.

The NeuN labeling showed good preservation of ganglion cells until very late in the disease progression therefore investigating ganglion cells as potential target for optogenetic treatment would be of value.

During advanced stages of the disease the $CRX^{Rdy/+}$ cat develops a severe lesion in the *area centralis* region characterized by RPE loss. Some islands of RPE hypertrophy were also seen. The mechanism of RPE degeneration in the macula-like region of the $CRX^{Rdy/+}$ cat warrants further investigation to determine the underlying causal factors and molecular mechanism. Also we need to investigate if it is a consequence of the dominant negative effect of the CRX mutant allele or due to the retinal degeneration and its molecular consequences (Veleri et al., 2015). The possibility that the $CRX^{Rdy/+}$ cat be a good model for RPE atrophy mechanistic studies in inherited disease or age macular degeneration is of importance (Green, 1999; Ramkumar et al., 2010).

This study showed that retinal degeneration in the $CRX^{Rdy/+}$ cat retina follows the 3 proposed phases of retinal remodeling. As early as 12 weeks of age, some glial reaction to photoreceptor death was observed this progressed leading to formation of a glial seal. In addition, there was neuronal rewiring and inner nuclear layer cell migration. Finally, microneuroma formation, severe retinal thinning and

A. Fundus images



B. Retinal pigmentary epithelium changes

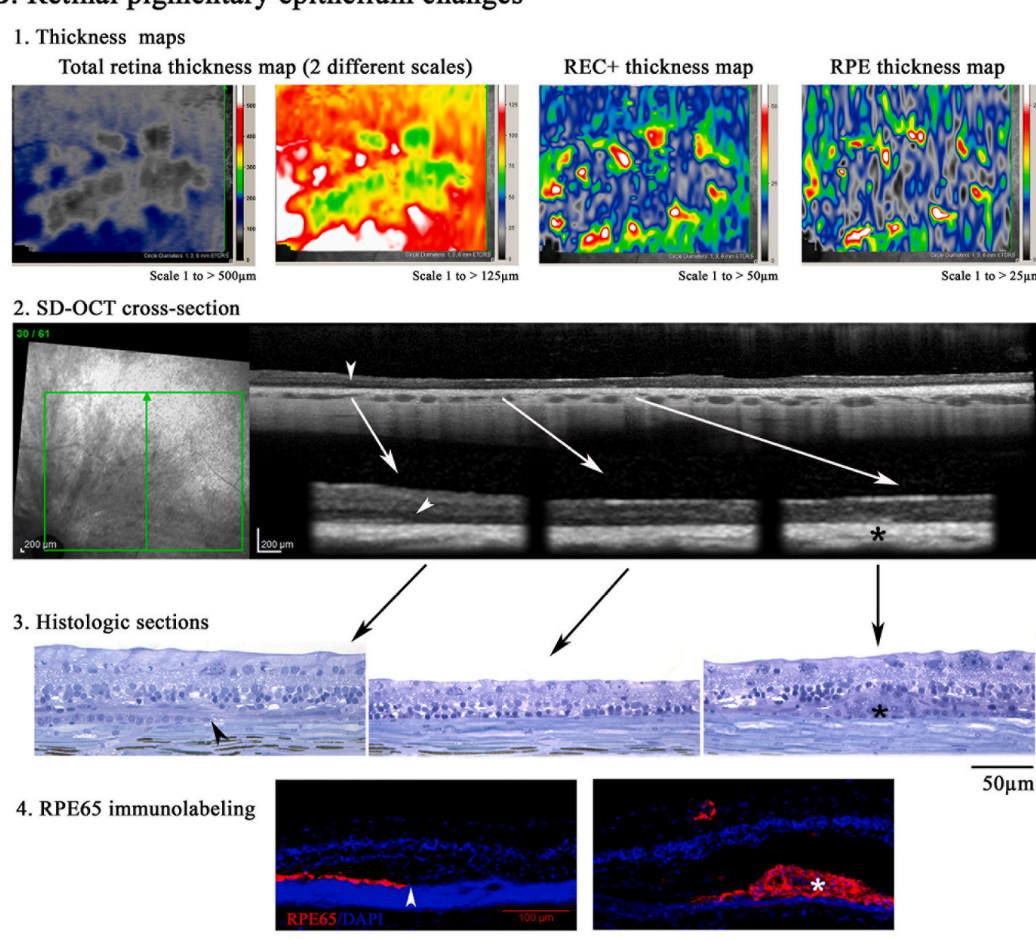


Fig. 7. Area centralis lesion in a 6.5-year-old $CRX^{Rdy/+}$ cat. **(A) Fundus images** indicating the lesion in the area centralis (black arrows). The lesion has a bluish appearance on the color fundus images, darker appearance on IR cSLO and shows some loss of autofluorescence on FAF (also see Fig. 1). Fluorescein angiography shows lack of fluorescence in the region of the area centralis and its surroundings indicated loss of the RPE. Note that there is some fluorescein leakage from retinal vasculature. (B) Retinal layer thickness in the region of the RPE lesion. **1.** Thickness maps in the area of the lesion show total retinal thinning (shown with two color scales) and thinning of the REC+. Interesting the RPE layer is thinned but there are also some focal regions of thickening (green to red color are seen in the edges of the lesion. Those corresponded on retinal cross sections (2) to an RPE thickening (right panel), seen as RPE cell proliferation as seen on histologic and immunolabeled sections (2,3,4: black and white stars). The center of the lesion is thin and has a lack of RPE layer (central panels; 3,4). The region where the integrity of the RPE stops can be seen on SD-OCT, histologic section and IHC (white and black arrowheads; left panels; 2,3,4).

remodeling developed. These findings may provide potential limitation of therapies such as optogenetics or retinal transplant to earlier stage disease such as under 1.5-years of age to ensure a potentially responsive neuronal environment at the time of treatment. Adding to the previous

description of the CRX^{Rdy} phenotype these findings provide baseline information for planned therapeutic interventions and evaluation. The CRX^{Rdy} cat is a valuable large animal model for studying the severe forms of Leber congenital amaurosis due to CRX mutations but also

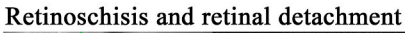
A. Dorsal lesions

Bullous elevation and vessel leakage

Retinal hypertrophy in the dorsal periphery

Tapetal atrophy

B. Ventral lesions
Retinal holes



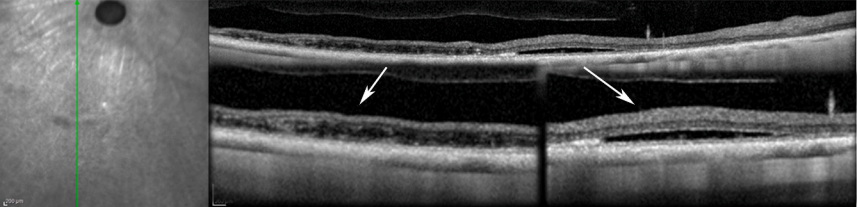


Fig. 8. Additional lesions observed in the older $CRX^{Rdy/+}$ cat. **(A) Dorsal lesions** - bullous elevation of the retina (*black arrowheads*) with internal limiting membrane detachments were detected. Some retinal hypertrophy was noticed in the far dorsal periphery and some tapetal atrophy was randomly found (seen as a lack of tapetal autofluorescence on IHC). **(B) Ventral lesions** – these included presence of retinal holes (*white arrowheads*) in very advanced degeneration cases and one cat presented with bilateral retinoschisis (*white arrow* left panel) and retinal detachments (*white arrow* right panel).

retinal neuronal remodeling and degeneration and RPE atrophy.

Funding

This work was supported by National Institutes Health [grant numbers EY015128 (BWJ), EY028927 (BWJ), EY014800 to core (BWJ)], National Science Foundation [grant number NN2 2014862 to (BWJ)], a Research to Prevent Blindness (New York) Unrestricted Grant to the Department of Ophthalmology & Visual Sciences, University of Utah, and an unrestricted grant from Gabe Newell (BWJ), Myers Dunlap Endowment (SMPJ), George H. Bird and "Casper" Endowment for Feline Initiatives (LMO and SMPJ), MSU Center for Feline Health and Well Being (LMO and SMPJ).

Data availability

Data will be made available on request.

Acknowledgements

The authors would like to thank Dr Alicia Withrow for her help with semithin sections, Wenjuan Ma from MSU CSTAT for her help with statistical analysis, Dr Cheryl Craft for the donation of the hCAR antibody, Dr Debra Thompson for the donation of RPE65 antibody and Janice Querubin for help with animal anesthesia.

Appendix A. Supplementary data

Supplementary data to this article can be found online at https://doi. org/10.1016/j.exer.2023.109630.

References

Chong, N.H., Alexander, R.A., Barnett, K.C., Bird, A.C., Luthert, P.J., 1999. An immunohistochemical study of an autosomal dominant feline rod/cone dysplasia (Rdy cats). Exp. Eye Res. 68, 51–57.

- Curtis, R., Barnett, K.C., Leon, A., 1987. An early-onset retinal dystrophy with dominant inheritance in the Abyssinian cat. Clinical and pathological findings. Invest. Ophthalmol. Vis. Sci. 28, 131–139.
- Freund, C.L., Gregory-Evans, C.Y., Furukawa, T., Papaioannou, M., Looser, J., Ploder, L., Bellingham, J., Ng, D., Herbrick, J.A.S., Duncan, A., Scherer, S.W., Tsui, L.C., Loutradis-Anagnostou, A., Jacobson, S.G., Cepko, C.L., Bhattacharya, S.S., McInnes, R.R., 1997. Cone-rod dystrophy due to mutation in a novel photoreceptor-specific homeobox gene (CRX) essential for maintenance of the photoreceptor. Cell 91, 543–553.
- Furukawa, T., Morrow, E.M., Li, T., Davis, F.C., Cepko, C.L., 1999. Retinopathy and attenuated circadian entrainment in Crx-deficient mice. Nat. Genet. 23, 466–470.
- Green, W.R., 1999. Histopathology of age-related macular degeneration. Mol. Vis. 5, 27. Hennig, A.K., Peng, G.H., Chen, S., 2008. Regulation of photoreceptor gene expression by Crx-associated transcription factor network. Brain Res. 1192, 114–133.
- Hood, D.C., Lin, C.E., Lazow, M.A., Locke, K.G., Zhang, X., Birch, D.G., 2009. Thickness of receptor and post-receptor retinal layers in patients with retinitis pigmentosa measured with frequency-domain optical coherence tomography. Invest.
- Ophthalmol. Vis. Sci. 50, 2328–2336.

 Huang, L., Xiao, X., Li, S., Jia, X., Wang, P., Guo, X., Zhang, Q., 2012. CRX variants in cone-rod dystrophy and mutation overview. Biochem. Biophys. Res. Commun. 426,
- Itabashi, T., Wada, Y., Sato, H., Kawamura, M., Shiono, T., Tamai, M., 2004. Novel 615delC mutation in the CRX gene in a Japanese family with cone-rod dystrophy. Am. J. Ophthalmol. 138, 876–877.
- Itabashi, T., Wada, Y., Sato, H., Kunikata, H., Kawamura, M., Tamai, M., 2003. Ocular findings in a Japanese family with an Arg41Trp mutation of the CRX gene. Graefes Arch. Clin. Exp. Ophthalmol. 241, 535–540.
- Jones, B.W., Kondo, M., Terasaki, H., Lin, Y., McCall, M., Marc, R.E., 2012. Retinal remodeling. Jpn. J. Ophthalmol. 56, 289–306.
- Jones, B.W., Marc, R.E., 2005. Retinal remodeling during retinal degeneration. Exp. Eye Res. 81, 123–137.
- Jones, B.W., Pfeiffer, R.L., Ferrell, W.D., Watt, C.B., Marmor, M., Marc, R.E., 2016a. Retinal remodeling in human retinitis pigmentosa. Exp. Eye Res. 150, 149–165.
- Jones, B.W., Pfeiffer, R.L., Ferrell, W.D., Watt, C.B., Tucker, J., Marc, R.E., 2016b. Retinal remodeling and metabolic alterations in human AMD. Front. Cell. Neurosci. 10, 103.
- Jones, B.W., Watt, C.B., Frederick, J.M., Baehr, W., Chen, C.K., Levine, E.M., Milam, A. H., LaVail, M.M., Marc, R.E., 2003. Retinal remodeling triggered by photoreceptor degenerations. J. Comp. Neurol. 464, 1–16.
- Leon, A., Curtis, R., 1990. Autosomal dominant rod-cone dysplasia in the Rdy cat. 1. Light and electron microscopic findings. Exp. Eye Res. 51, 361–381.
- Leon, A., Hussain, A.A., Curtis, R., 1991. Autosomal dominant rod-cone dysplasia in the Rdy cat. 2. Electrophysiological findings. Exp. Eye Res. 53, 489–502.
- Marc, R.E., Jones, B.W., 2002. Molecular phenotyping of retinal ganglion cells. J. Neurosci. 22, 413–427.
- Marc, R.E., Jones, B.W., 2003. Retinal remodeling in inherited photoreceptor degenerations. Mol. Neurobiol. 28, 139–147.

- Marc, R.E., Jones, B.W., Watt, C.B., Strettoi, E., 2003. Neural remodeling in retinal degeneration. Prog. Retin. Eye Res. 22, 607–655.
- Marc, R.E., Murry, R.F., Basinger, S.F., 1995. Pattern recognition of amino acid signatures in retinal neurons. J. Neurosci. 15, 5106–5129.
- Marc, R.E., Murry, R.F., Fisher, S.K., Linberg, K.A., Lewis, G.P., 1998a. Amino acid signatures in the detached cat retina. Invest. Ophthalmol. Vis. Sci. 39, 1694–1702.
- Marc, R.E., Murry, R.F., Fisher, S.K., Linberg, K.A., Lewis, G.P., Kalloniatis, M., 1998b.
 Amino acid signatures in the normal cat retina. Invest. Ophthalmol. Vis. Sci. 39, 1685–1693.
- Menotti-Raymond, M., Deckman, K.H., David, V., Myrkalo, J., O'Brien, S.J., Narfstrom, K., 2010. Mutation discovered in a feline model of human congenital retinal blinding disease. Invest. Ophthalmol. Vis. Sci. 51, 2852–2859.
- Mowat, F.M., Gornik, K.R., Dinculescu, A., Boye, S.L., Hauswirth, W.W., Petersen-Jones, S.M., Bartoe, J.T., 2014. Tyrosine capsid-mutant AAV vectors for gene delivery to the canine retina from a subretinal or intravitreal approach. Gene Ther. 21, 96–105.
- Nishiguchi, K.M., Kunikata, H., Fujita, K., Hashimoto, K., Koyanagi, Y., Akiyama, M., Ikeda, Y., Momozawa, Y., Sonoda, K.H., Murakami, A., Wada, Y., Nakazawa, T., 2020. Association of CRX genotypes and retinal phenotypes confounded by variable expressivity and electronegative electroretinogram. Clin. Exp. Ophthalmol. 48, 644-657
- Occelli, L.M., Pirie, C.G., Petersen-Jones, S.M., 2022. Non-invasive optical coherence tomography angiography: a comparison with fluorescein and indocyanine green angiography in normal adult dogs and cats. Vet. Ophthalmol. 25 (Suppl. 1), 164-178
- Occelli, L.M., Tran, N.M., Narfstrom, K., Chen, S., Petersen-Jones, S.M., 2016. CrxRdy cat: a large animal model for CRX-associated leber congenital amaurosis. Invest. Ophthalmol. Vis. Sci. 57, 3780–3792.
- Pfeiffer, R.L., Anderson, J.R., Emrich, D.P., Dahal, J., Sigulinsky, C.L., Morrison, H.A.B., Yang, J.H., Watt, C.B., Rapp, K.D., Kondo, M., Terasaki, H., Garcia, J.C., Marc, R.E., Jones, B.W., 2019. Pathoconnectome analysis of müller cells in early retinal remodeling. Adv. Exp. Med. Biol. 1185, 365–370.
- Pfeiffer, R.L., Marc, R.E., Jones, B.W., 2020. Müller cell metabolic signatures: evolutionary conservation and disruption in disease. Trends Endocrinol. Metabol. 31, 320–329.
- Pfeiffer, R.L., Marc, R.E., Kondo, M., Terasaki, H., Jones, B.W., 2016. Müller cell metabolic chaos during retinal degeneration. Exp. Eve Res. 150, 62–70.
- metabolic chaos during retinal degeneration. Exp. Eye Res. 150, 62–70. Ramkumar, H.L., Zhang, J., Chan, C.C., 2010. Retinal ultrastructure of murine models of dry age-related macular degeneration (AMD). Prog. Retin. Eye Res. 29, 169–190.
- RStudio Team, 2015. RStudio. Integrated Development for R. RStudio, I., Boston, MA. URL. http://www.rstudio.com/.
- Tran, N.M., Chen, S., 2014. Mechanisms of blindness: animal models provide insight into distinct CRX-associated retinopathies. Dev. Dynam. 243, 1153–1166 an official publication of the American Association of Anatomists.
- Veleri, S., Lazar, C.H., Chang, B., Sieving, P.A., Banin, E., Swaroop, A., 2015. Biology and therapy of inherited retinal degenerative disease: insights from mouse models. Dis Model Mech 8, 109–129.